

Supplementary Material

Multiday haze in the East Asia: Transport and chemical aging

Yong Bin Lim, Jihoon Seo, Jin Young Kim and Barbara J. Turpin

S1 (Text)	Page S 2-3
Figure S1	Page S 4
Figure S2	Page S 5
Figure S3	Page S 6
Figure S4	Page S 7
Figure S5	Page S 8
Figure S6	Page S 9
Table S1	Page S 10
Table S2	Page S 11
Table S3	Page S 12
References	Page S 13

S1. ALW, pH, and NO_3^- estimation

For smog chamber aerosols, Model II of Extended-Aerosol Inorganic Model (*E*-AIM) (Wexler and Clegg, 2002) was used. The effective Henry's law constant for glyoxal ($2 \times 10^7 \text{ M/atm}$) was used. Neither radical nor non-radical reactions was considered. Measurements of species ($\mu\text{g}/\text{m}^3$) were converted to moles per the unit volume (moles/ m^3). The input for H^+ (or OH^-) was determined by the ion balance method (Hennigan et al., 2015):

$$\sum n_i \times [\text{Anion}]_i - \sum n_i \times [\text{Cation}]_i = [\text{H}^+] \quad (\text{Eq. S2-1})$$

$$\sum n_i \times [\text{Cation}]_i - \sum n_i \times [\text{Anion}]_i = [\text{OH}^-] \quad (\text{Eq. S2-2})$$

where n_i is a stoichiometric coefficient of species, *i*.

$[\text{ALW}]_i$ and pH_i in Supplementary Table 1 are estimated by *E*-AIM under the conditions above (inputs). Since the mass increase was only due to water uptake, $[\text{ALW}]_f$ was obtained as follows:

$$[\text{ALW}]_f = [\text{ALW}]_i + ([\text{M}]_f' - [\text{M}]_i) \quad (\text{Eq. S3})$$

where $[\text{M}]_f'$ is the wall loss corrected $[\text{M}]_f$, which was measured by SMPS.

To determine pH_f and $[\text{NO}_3^-]$ after smog chamber reactions (Table S1), an equilibrium model was developed by using FACSIMILE (MCPA Software Ltd.) that contained equilibria listed in Table S3. It was assumed that all NO_2 became HNO_3 by OH oxidation in the gas phase. Concentrations were corrected by accounting ALW_f . In addition to the concentration of NO_3^- , concentrations of inorganic constituents in wet aerosols are listed in Table S2.

To determine concentrations of organic/inorganic constituents, ALW, and pH of haze particles in the atmosphere, off-line measurements by GC-MS needed to be corrected for water uptake by *E*-AIM Model IV. Glyoxal was used as a surrogate of organic compounds (Brooks et al., 2002). The daytime humidity during the haze event in Seoul varied from ~ 70 % RH in the morning (8 AM)

to ~ 35 % RH in the afternoon (3 PM) (Fig S6). So, 70 % RH was used in *E-AIM*. Note that the photooxidation in the smog chamber also started at ~ 70 % RH (Fig. S1). No overcast weather was observed during the haze event. The average temperature (5°C) was used in *E-AIM*. In addition to *E-AIM* estimation of the concentration of NO_3^- based on NO_3^- measurements on filters. We also estimates the concentration of NO_3^- through the Henry's law equilibrium from HNO_3 in the gas phase using the equilibrium model. The average temperature (5°C) was also used. Estimated concentrations of NO_3^- , and other organic/inorganic constituents by the equilibrium model are listed in Table S2.

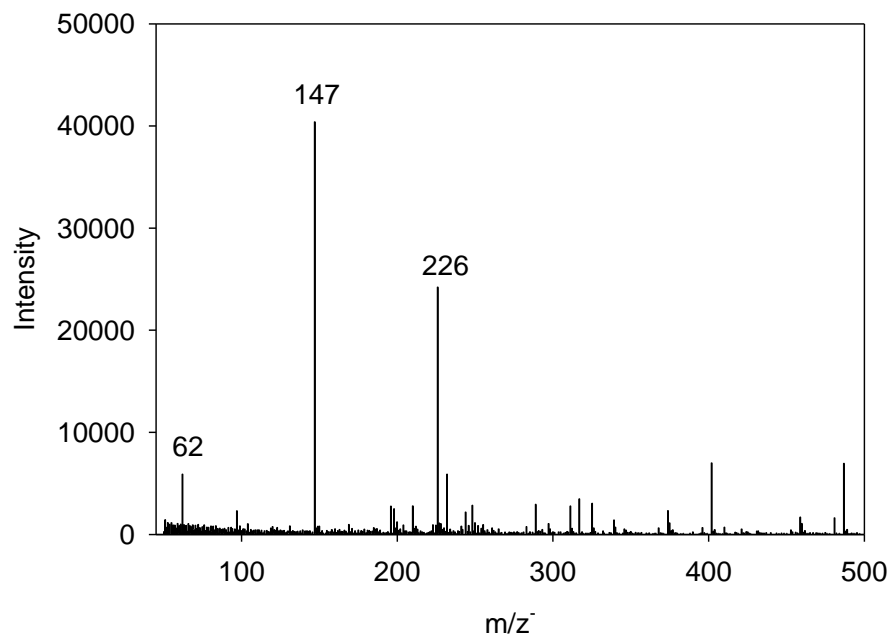


Fig. S1. A negative mode of UPLC-Q-TOF-mass spectrum for a pure HNO_3 solution (1.5 mM). m/z^- 147 and 226 are nitrate clusters (m/z^- 62 is a nitrate). m/z^- 147 (146.9653) represents $[\text{Na}(\text{NO}_3)_2]^-$ with the uncertainty of 4.5 ppm. m/z^- 226 (225.9278) represents $[\text{Ca}(\text{NO}_3)_3]^-$ with the uncertainty of 10.2 ppm.

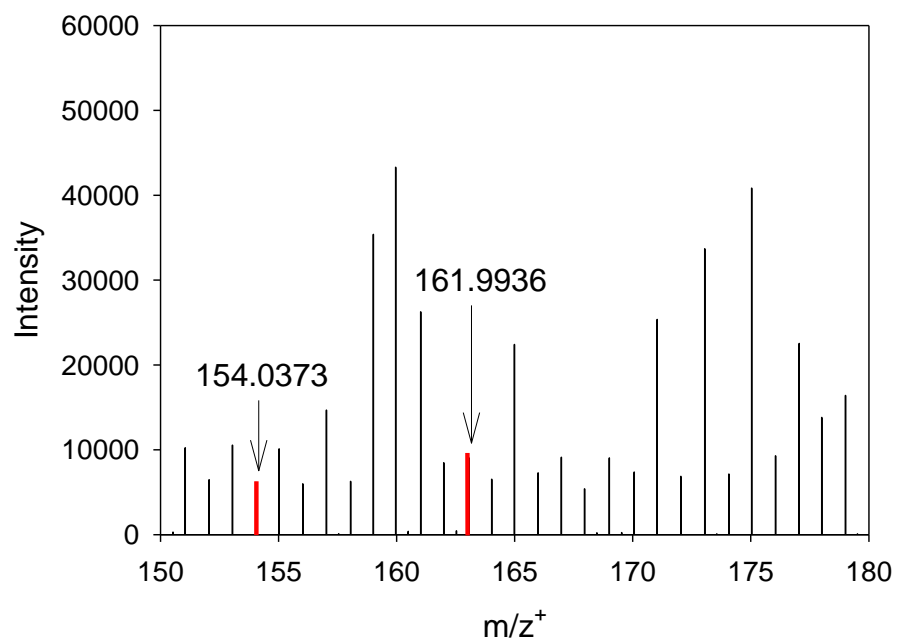


Fig. S2. A positive mode of HR-Q-TOF-mass spectrum for a standard mixture solution of glyoxal (3.8 mM) and HNO₃ solution (15 mM).

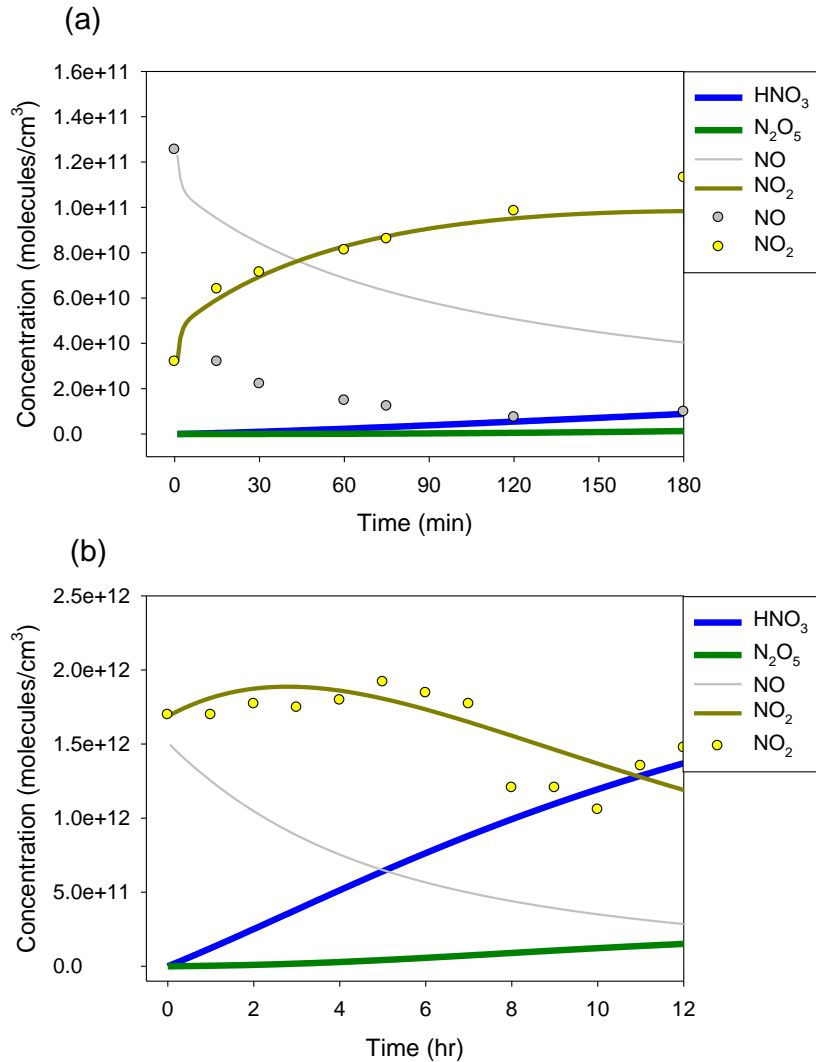


Fig. S3. Photochemical Model simulations for HNO_3 , N_2O_5 and NO_x , and measurements for NO_x . (a) is under chamber conditions. (b) is under ambient conditions. Gas-phase $\text{NO}_x\text{-HO}_x$ chemistry model has been developed here based on the Lim cloud model (Lim et al., 2005). The actinometric experiments for lamps in our chamber determine that the photolysis rate of NO_2 is 0.55 min^{-1} (Lee, 2007). For chamber simulations, the concentration of OH radicals is $1\text{e}6 \text{ molecules cm}^{-3}$. The conversion rate of NO to NO_2 by peroxy radicals is set to be $1\text{-}11 \text{ cm}^3 \text{ molecules}^{-1} \text{ s}^{-1}$ – Note that the conversion rate for $\text{C}_2\text{H}_5\text{OO}\bullet$ is $9.1\text{e-}12 \text{ cm}^3 \text{ molecules}^{-1} \text{ s}^{-1}$ (Atkinson et al., 2006). The OH reaction rate of VOC, which is the source of peroxy radicals that convert NO to NO_2 , is set to be $5\text{e-}10 \text{ cm}^3 \text{ molecules}^{-1} \text{ s}^{-1}$ – Note that the OH rate for formic acid (presumably evaporated organic compounds from aqueous OH reaction of glyoxal) is $\sim 3\text{e-}10 \text{ cm}^3 \text{ molecules}^{-1} \text{ s}^{-1}$ (Kwok and Atkinson, 1995). For ambient simulation, the photolysis rate of NO_2 is set to be 0.27 min^{-1} (Lim et al., 2005). The concentration of OH radicals is $1\text{e}6 \text{ molecules cm}^{-3}$. Other parameters are set to be the same as chamber conditions. Note that $[\text{NO}]$ is overestimated under chamber conditions (a) (the possible sink of NO to the wall loss as HONO), and no ambient $[\text{NO}]$ is available during the multiday haze event (b).

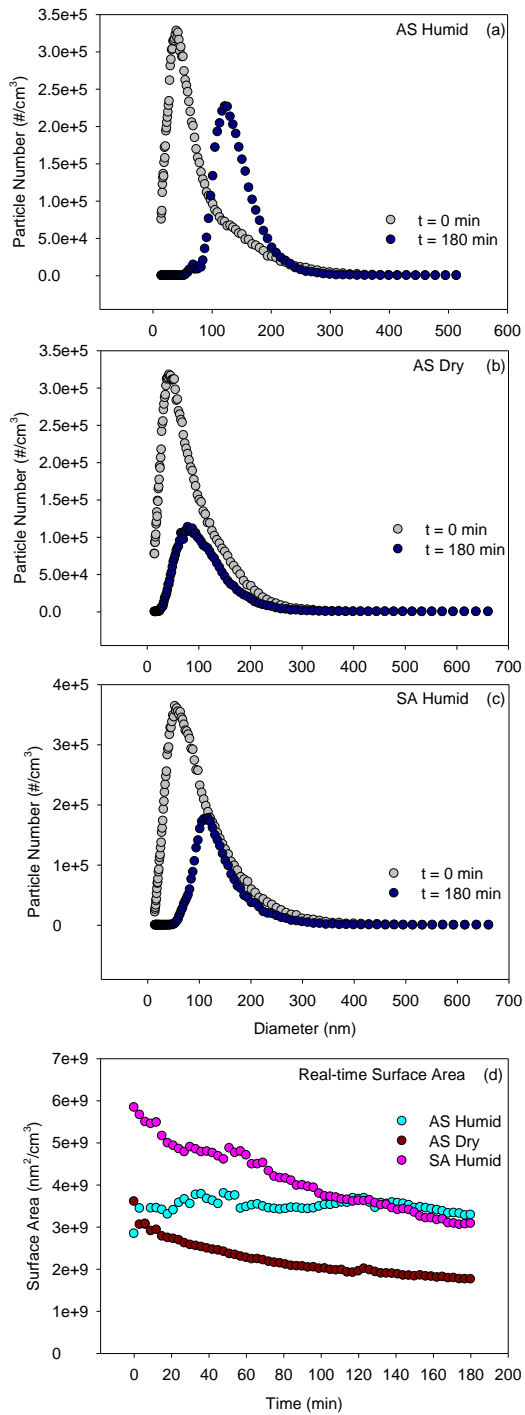


Fig. S4. Particle number distributions of AS aerosols in the humid chamber (a), AS aerosols in the dry chamber (b), and SA aerosols in the humid chamber (c) at $t = 0$ min and $t = 180$ min (a, b, and c); surface area distributions AS and SA aerosols in the humid/dry chamber during 3 hour photooxidation (d). Only (a) represents the condensation of water vapor and the coagulation while (b), (c), and (d) represent only the coagulation. Consequently, the surface area for AS humid is the constant while the other surface areas for AS dry and SA humid decrease.

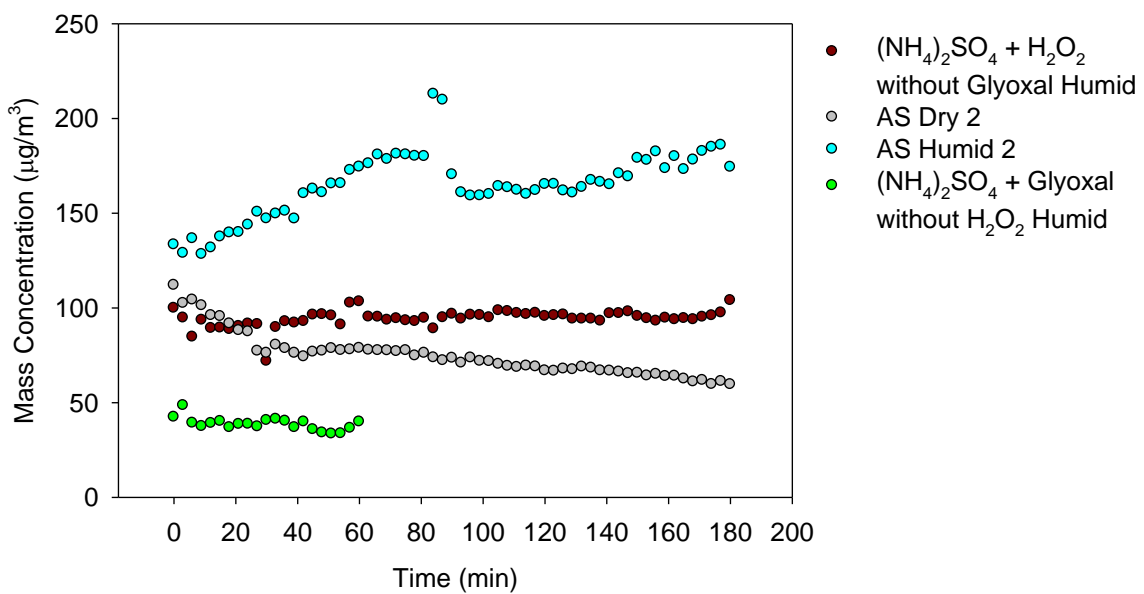


Fig. S5. 1) AS aerosols in the absence of glyoxal in the humid chamber (●); 2) AS aerosols in the dry chamber (○); 3) AS aerosols in the humid chamber (○); and 4) AS aerosols in the absence of H_2O_2 in the humid chamber (●). All of plots were wall-loss corrected.

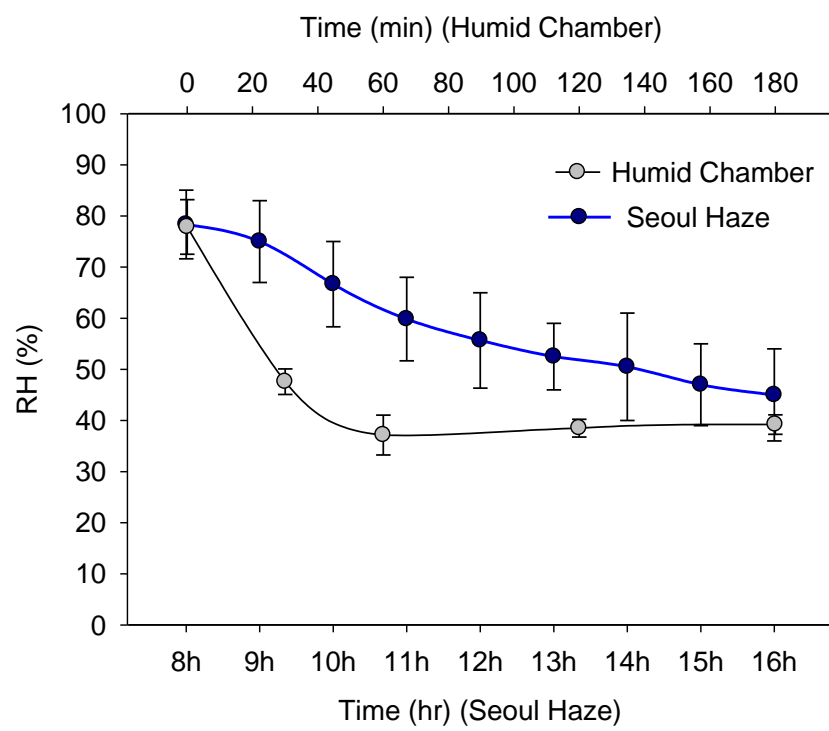


Fig. S6. Average daytime variations of RH during the haze event in Seoul (Seoul Haze) and average RH variations during the photooxidation in the humid condition (Humid Chamber)

Table S1. Smog chamber experimental conditions

#	Atomized Solution Date	UV or Dark	RH _i (%)	RH _f (%)	T _i (K)	T _f (K)	[NO] _i (ppb)	[NO] _f (ppb)	[O ₃] _i (ppb)	[O ₃] _f (ppb)	[M] _i (µg/m ³)	[M] _f (µg/m ³)	[M] _{f'} (µg/m ³)	[ALW] _i (µg/m ³)	[ALW] _f (µg/m ³)	[NO ₃ ⁻] (M)
							[NO _x] _i (ppb)	[NO _x] _f (ppb)						pH _i	pH _f	
1	AS + H ₂ O ₂ + Gly 3/5/2015	UV	3.0	3.0	293	303	24.0	5.5	0	24.9	76.2	47.7	61.3	0.8	-	-
							28.0	25.5						6.4		
2	AS + H ₂ O ₂ + Gly 3/31/2015	UV	3.0	3.0	294	309	8.2	4.4	6.9	7.7	77.7	32.9	63.6	0.8	-	-
							9.4	15.6						6.4		
3	AS + H ₂ O ₂ + Gly 11/26/2015	UV	3.0	3.0	292	306	2.4	0	9.6	34.0	87.5	40.0	75.2	0.9	-	-
							2.9	1.1						6.4		
4	AS + H ₂ O ₂ + Gly 3/23/2015	UV	70.8	38.9	294	304	5.1	0.4	7.4	11.3	73.2	101.4	157.4	34.7	117.7	0.9
							6.4	4.6						4.8		
5	AS + H ₂ O ₂ + Gly 4/1/2015	UV	82.2	42.0	295	310	7.2	2.7	6.9	15.4	131.6	96.5	161.7	77.9	108.0	1.0
							10.5	7.4						4.6		
6	AS + Gly 5/27/2015	UV*	69.4	34.8	298	310	54.7	23.3	13.0	18.0	41.3	26.3	39.8	19.0	16.8	-
							55.5	38.7						4.7		
7	AS + H ₂ O ₂ 3/30/2015	UV	83.7	39.1	295	310	8.5	3.2	7.6	12.1	98.8	61.9	91.3	60.5	55.0	-
							11.7	7.1						4.5		
8	AS + H ₂ O ₂ + Gly 4/27/2015	Dark	3.0	3.0	297	297	17.2	17.2	6.4	5.9	72.2	33.5	76.5	0.6	-	-
							19.1	17.1						6.3		
9	AS + H ₂ O ₂ + Gly 4/28/2015	Dark	77.7	56.2	298	298	38.9	27.8	6.2	7.8	42.5	22.6	38.5	22.9	18.9	-
							39.9	33.2						4.6		
10	AS + H ₂ O ₂ + Gly 5/7/2015	Dark	71.7	64.9	298	298	15.8	15.6	5.6	6.3	225.1	42.9	194.0	108.3	74.0	-
							16.9	17.1						4.7		
11	SA + H ₂ O ₂ + Gly 3/9/2015	UV	7.1	3.0	293	304	80.9	41.6	0	7.7	99.3	36.9	96.3	32.1	29.1	4.9e-3
							83.5	77.7						-1.1		
12	SA + H ₂ O ₂ + Gly 3/25/2015	UV	82.0	44.8	294	307	21.6	15.2	6.2	8.5	174.1	67.5	154.5	129.2	109.6	1.4e-3
							23.9	19.7						-0.6		
13	SA + H ₂ O ₂ + Gly 5/6/2015	Dark	3.0	3.0	298	298	15.8	15.6	5.6	6.3	31.4	15.9	35.8	8.4	-	-
							16.9	17.1						-1.1		
14	SA + H ₂ O ₂ + Gly 4/29/2015	Dark	77.6	77.1	298	298	15.8	15.7	6.1	6.3	88.5	49.4	87.3	62.7	63.9	-
							18.0	17.5						-0.7		

Note, AS = ammonium sulfate, SA = sulfuric acid, AN = Ammonium Nitrate, Gly = glyoxal, i = initial, f = final, M = particle, [M]_f = uncorrected mass concentration, [M]_{f'} = wall loss corrected mass concentration, [NO₃⁻] = nitrate concentration formed in particles after the chamber reaction, and ALW = aerosol liquid water. UV* indicates 1-hour irradiation. “-” indicates no ALW.

Table S2. Concentrations of organic and inorganic constituents and pH in wet aerosols

	NO_3^-	NH_4^+	HSO_4^-	SO_4^{2-}	Organic Compounds	pH
Exp 4	1.54 M	4.03 M	1.48 M	0.53 M	0.17 M	1.3
Exp 5	2.05 M	5.71 M	2.01 M	0.86 M	0.24 M	1.3
Seoul Haze	3.30 M	7.49 M	0.30 M	2.02 M	2.08 M	1.2
Seoul Clean	2.36 M	4.64 M	0 M	1.29 M	4.92 M	8.7
Deokjeok Island Haze	1.74 M	6.94 M	0 M	2.69 M	2.79 M	8.9
Deokjeok Island Clean	1.76 M	5.51 M	0 M	2.20 M	3.78 M	9.0

Table S3. Aqueous-phase reactions after HNO_3 uptake

	Reactions	K_{298} (M/atm or M)	$-\Delta H/R$ (K)	Ref
1	$\text{HNO}_{3g} \rightleftharpoons \text{HNO}_3$	$K_{eq} = 1.6e5$ M/atm	8700	(Warneck, 1999)
2	$\text{HNO}_3 \rightleftharpoons \text{H}^+ + \text{NO}_3^-$	$K_{eq} = 15.4$ M	N/A	(Seinfeld and Pandis, 2016)
3	$\text{H}_2\text{SO}_4 \rightleftharpoons \text{H}^+ + \text{HSO}_4^-$	$K_{eq} = 1e3$ M	N/A	(Seinfeld and Pandis, 2016)
4	$\text{HSO}_4^- \rightleftharpoons \text{H}^+ + \text{SO}_4^{2-}$	$K_{eq} = 1.02e-2$ M	2720	(Lim et al., 2005)
5	$\text{NH}_4\text{OH} \rightleftharpoons \text{NH}_4^+ + \text{OH}^-$	$K_{eq} = 1.7e-5$ M	-450	(Seinfeld and Pandis, 2016)
6	$\text{H}_2\text{O} \rightleftharpoons \text{H}^+ + \text{OH}^-$	$K_{eq} = 1.0e-14$ M	-6710	(Seinfeld and Pandis, 2016)

$$K(T) = K_{298} \exp \left[-\frac{\Delta H}{R} \left(\frac{1}{T} - \frac{1}{298} \right) \right]$$

$K(T)$ is a temperature dependent equilibrium constant. K_{298} is an equilibrium constant at 298K.

N/A indicates $K(T) = K_{298}$.

References

Atkinson, R., Baulch, D. L., Cox, R. A., Crowley, J. N., Hampson, R. F., Hynes, R. G., Jenkin, M. E., Rossi, M. J., and Troe, J.: Evaluated kinetic and photochemical data for atmospheric chemistry: Volume II - gas phase reactions of organic species, *Atmos. Chem. Phys.*, 6, 3625-4055, 2006.

Brooks, S. D., Wise, M. E., Cushing, M., and Tolbert, M. A.: Deliquescence behavior of organic/ammonium sulfate aerosol, *Geophys Res Lett*, 29, 23-21-23-24, 10.1029/2002GL014733, 2002.

Hennigan, C. J., Izumi, J., Sullivan, A. P., Weber, R. J., and Nenes, A.: A critical evaluation of proxy methods used to estimate the acidity of atmospheric particles, *Atmos. Chem. Phys.*, 15, 2775-2790, 10.5194/acp-15-2775-2015, 2015.

Kwok, E. S. C., and Atkinson, R.: Estimation of Hydroxyl Radical Reaction-Rate Constants for Gas-Phase Organic-Compounds Using a Structure-Reactivity Relationship - an Update, *Atmos. Environ.*, 29, 1685-1695, Doi 10.1016/1352-2310(95)00069-B, 1995.

Lee, S.-B.: Formation and growth of secondary particles during photochemical reactions of ambient air - effects of light intensity, ambient aerosols, and diesel exhaust aerosols, Ph.D., School of Mechanical and Aerospace Engineering, Seoul National University, 183 pp., 2007.

Lim, H. J., Carlton, A. G., and Turpin, B. J.: Isoprene forms secondary organic aerosol through cloud processing: Model simulations, *Environ. Sci. Technol.*, 39, 4441-4446, 10.1021/es048039h, 2005.

Seinfeld, J. H., and Pandis, S. N.: Atmospheric chemistry and physics: from air pollution to climate change, 3rd ed., John Wiley & Sons, 1152 pp., 2016.

Warneck, P.: The relative importance of various pathways for the oxidation of sulfur dioxide and nitrogen dioxide in sunlit continental fair weather clouds, *PCCP*, 1, 5471-5483, 10.1039/a906558j, 1999.

Wexler, A. S., and Clegg, S. L.: Atmospheric aerosol models for systems including the ions H^+ , NH_4^+ , Na^+ , SO_4^{2-} , NO_3^- , Cl^- , Br^- , and H_2O , *J. Geophys. Res. Atmos.*, 107, ACH 14-11-ACH 14-14, 10.1029/2001JD000451, 2002.